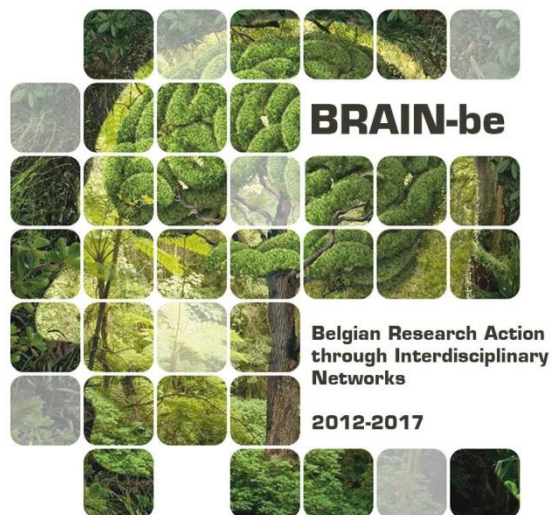


COME-IN

Constraining Mercury's Interior structure and evolution

Tim Van Hoolst (Royal Observatory of Belgium/KU Leuven) - Bernard Charlier (Université de Liège) - Stefaan Cottenier (Ghent University) - Wim van Westrenen (VU University Amsterdam, NL) - Olivier Namur (KU Leuven) - Attilio Rivoldini (Royal Observatory of Belgium) - Jurriën Knibbe (KU Leuven/Royal Observatory of Belgium) - Marie-Hélène Deproost (Royal Observatory of Belgium) - Jan Jaeken (Ghent University)

Axis 2: Geosystems, universe and climate



NETWORK PROJECT

COME-IN

Constraining Mercury's Interior structure and evolution

Contract - BR/143/A2/COME-IN

FINAL REPORT

PROMOTORS: Tim Van Hoolst (Royal Observatory of Belgium/KU Leuven)
Bernard Charlier (Université de Liège)
Stefaan Cottenier (Ghent University)
Wim van Westrenen (VU University Amsterdam, NL)
Olivier Namur (KU Leuven)

AUTHORS: Tim Van Hoolst (Royal Observatory of Belgium/KU Leuven)
Bernard Charlier (Université de Liège)
Stefaan Cottenier (Ghent University)
Wim van Westrenen (VU University Amsterdam, NL)
Olivier Namur (KU Leuven)
Marie-Hélène Deproost (Royal Observatory of Belgium)
Jan Jaeken (Ghent University)
Jurriën Knibbe (KU Leuven/ Royal Observatory of Belgium)
Attilio Rivoldini (Royal Observatory of Belgium)

| | | |
|---|---|--|
|  |  | |
|  |  | |
|  |  | |

Published in 2019 by the Belgian Science Policy Office
WTCIII
Simon Bolivarlaan 30 Boulevard Simon Bolivar
B-1000 Brussels
Belgium
Tel: +32 (0)2 238 34 11 - Fax: +32 (0)2 230 59 12
<http://www.belspo.be>
<http://www.belspo.be/brain-be>

Contact person: David Cox - Koen Lefever
Tel: +32 (0)2 238 34 03 - +32 (0)2 238 35 51

Neither the Belgian Science Policy Office nor any person acting on behalf of the Belgian Science Policy Office is responsible for the use which might be made of the following information. The authors are responsible for the content.

No part of this publication may be reproduced, stored in a retrieval system, or transmitted in any form or by any means, electronic, mechanical, photocopying, recording, or otherwise, without indicating the reference :

Tim Van Hoolst, Bernard Charlier, Stefaan Cottenier, Wim van Westrenen, Olivier Namur, Attilio Rivoldini, Jurriën Knibbe, Marie-Hélène Deproost, Jan Jaeken. *Constraining Mercury's Interior structure and evolution*. Final Report. Brussels : Belgian Science Policy Office 2019 – 33 p. (BRAIN-be - (Belgian Research Action through Interdisciplinary Networks))

TABLE OF CONTENTS

| | |
|---|-----------|
| ABSTRACT | 6 |
| 1. INTRODUCTION | 7 |
| 2. STATE OF THE ART AND OBJECTIVES | 8 |
| INTRODUCTION | 8 |
| 2.1 PRIMORDIAL SILICATE METAL EQUILIBRATION | 9 |
| 2.1.1 Core-mantle partitioning of trace elements | 9 |
| 2.1.2 The FeS layer at the core-mantle boundary | 9 |
| 2.2 MANTLE-CRUST EVOLUTION | 9 |
| 2.2.1 Mantle melting conditions | 9 |
| 2.2.2 Mineralogy of the mantle and the crust | 10 |
| 2.2.3 Crust density | 10 |
| 2.3 CORE STRUCTURE | 10 |
| 2.3.1 Density and VP measurements of Fe-Si liquids at high pressure | 10 |
| 2.3.2 Core heat budget | 10 |
| 2.3.3 Thermodynamic model of Fe-S-Si for the core | 11 |
| 2.3.4 Composition and layered structure of the inner core | 11 |
| 2.4 MODELS OF THE INTERIOR AND EVOLUTION | 11 |
| 2.4.1 Mercury's obliquity | 11 |
| 2.4.2 Global interior structure | 12 |
| 2.4.3 Global thermal evolution | 12 |
| 2.4.4 Mantle convection | 12 |
| 2.4.5 Rotational evolution | 12 |
| 3. METHODOLOGY, SCIENTIFIC RESULTS AND RECOMMENDATIONS | 13 |
| 3.1 PRIMORDIAL SILICATE METAL EQUILIBRATION | 13 |
| 3.1.1 Core-mantle partitioning of trace elements | 13 |
| 3.1.2 The FeS layer at the core-mantle boundary | 13 |
| 3.2 MANTLE-CRUST EVOLUTION | 14 |
| 3.2.1 Mantle melting conditions | 14 |
| 3.2.2 Mineralogy of the mantle and the crust | 14 |
| 3.2.3 Crust density and crustal production | 15 |
| 3.3 CORE STRUCTURE | 15 |
| 3.3.1 Density and VP measurements of Fe-Si liquids at high pressure | 15 |
| 3.3.2 Core heat budget | 16 |
| 3.3.3 Thermodynamic model of Fe-S-Si for the core | 19 |
| 3.3.4 Composition and layered structure of the inner core | 19 |
| 3.4 MODELS OF THE INTERIOR AND EVOLUTION | 20 |
| 3.4.1 Mercury's obliquity | 20 |
| 3.4.2 Global interior structure | 20 |

| | |
|--|-----------|
| 3.4.3 Global thermal evolution | 21 |
| 3.4.4 Mantle convection | 22 |
| 3.4.5 Rotational evolution | 22 |
| 4. DISSEMINATION AND VALORISATION | 24 |
| 5. PUBLICATIONS | 29 |
| 6. ACKNOWLEDGEMENTS | 33 |

ABSTRACT

Mercury has long been the least known of the terrestrial planets. Only two spacecraft have so far visited Mercury. Mariner10 flew by Mercury on three occasions in 1974-1975 and MESSENGER (MErcury Surface, Space ENvironment, GEochemistry and Ranging) orbited Mercury between 18 March 2011 and 30 April 2015. One of the primary goals of these missions is to gain a deeper understanding of the interior structure and evolution of this smallest terrestrial planet. Spacecraft measurements alone, however, are not sufficient to reach this goal. With COME-IN we aimed at advancing our understanding of Mercury by integrating complementary approaches from igneous petrology, high-pressure mineral physics, computational materials science, geodesy, and geodynamics in addition to using the constraints set by recent observational data. Building upon the complementary expertise of the five partners, we reached new and significant results on the primordial structure of Mercury after accretion, the magmatic processes relevant to the differentiation and evolution of Mercury, the physical properties and structure of the iron-rich core, and the global interior structure and thermal evolution of Mercury.

1. INTRODUCTION

This project focused on the interior of Mercury, the innermost planet of our Solar System (Fig. 1). It builds on the data from MESSENGER (MErcury Surface, Space ENvironment, GEochemistry, and Ranging), the first spacecraft to orbit the planet (2011-2015). In order to optimize the interpretation of these data in terms of the interior of Mercury, complementary laboratory experiments have been performed and theoretical modeling has been developed. This has been made possible by joining several (inter)national scientific teams, each active in Mercury research with a different but complementary expertise.

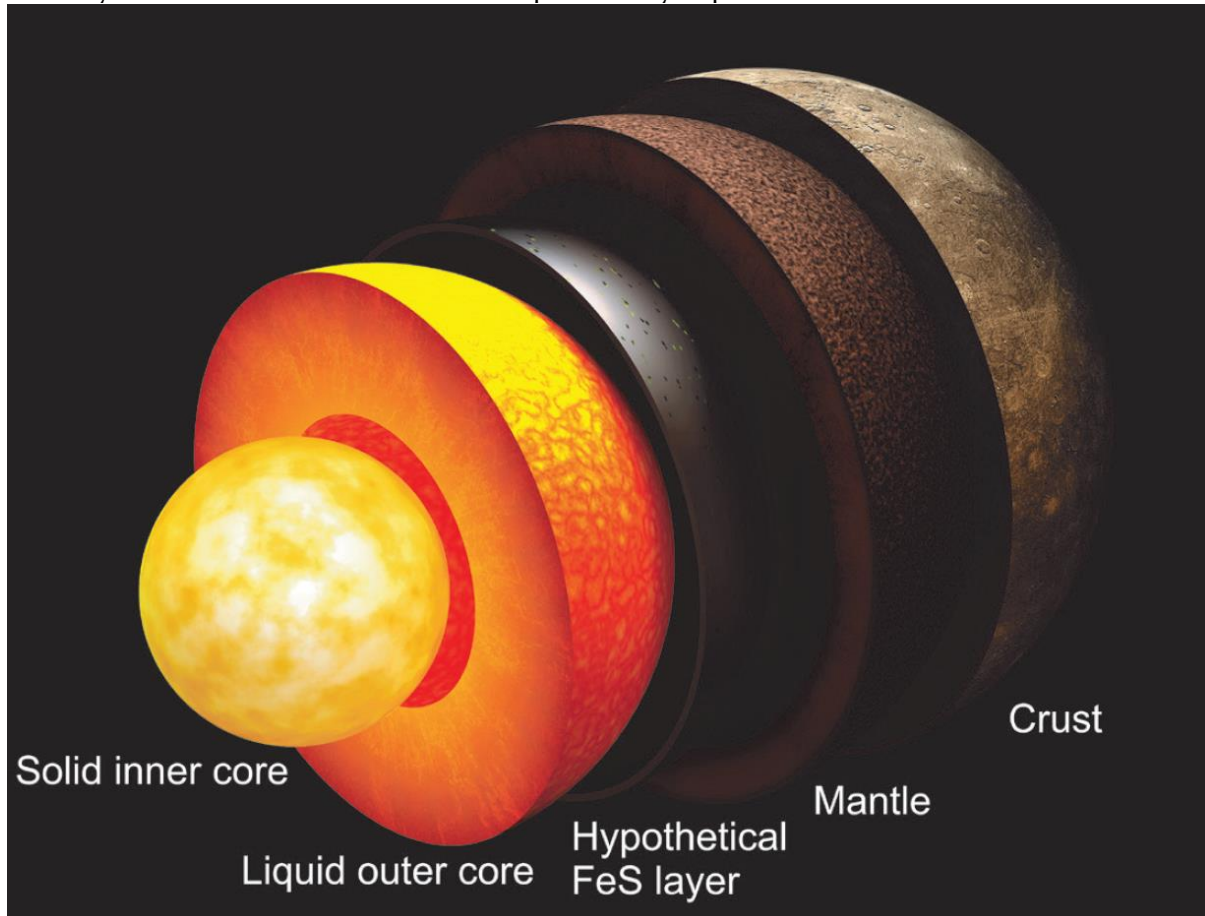


Figure 1: The interior structure of Mercury. The relatively thick crust (~40 km) overlies the comparatively thin mantle (~400 km). A hypothetical iron sulfide layer might occur at the core–mantle boundary, overlying the liquid outer core (radius of ~2,000 km). The innermost part of Mercury is probably a solid core having a radius of < 1,000 km (from Charlier and Namur 2019).

2. STATE OF THE ART AND OBJECTIVES

Introduction

Mercury has long been the least known of the terrestrial planets. Whereas Mars and Venus have been visited by several tens of spacecraft since the start of the space era, only two spacecraft have so far visited Mercury. Mariner10 flew by Mercury on three occasions in 1974-1975 and MESSENGER (MErcury Surface, Space ENvironment, GEochemistry and Ranging) orbited Mercury between 18 March 2011 and 30 April 2015. With the wealth of data gathered by the NASA MESSENGER spacecraft and the ESA/JAXA BepiColombo mission launched on 20 October 2018 and on schedule for Mercury orbit insertion in December 2025, the focus of the planetary science community on Mercury is stronger than ever. One of the primary goals of these missions to Mercury and of many theoretical, observational, and experimental studies is to gain a deeper understanding of the interior structure and evolution of this smallest terrestrial planet.

Several aspects of its composition and physical properties make Mercury unique among the terrestrial planets. Mercury is the only inner solar system body besides Earth with an active internally generated magnetic field, did not experience prolonged resurfacing and near-surface alteration on the scale experienced by Venus, Earth and Mars, and has an unusually high metal to silicate ratio. As such, Mercury holds the key to improved constraints on terrestrial planet formation processes in general, and on the early history of the inner parts of the solar nebula in particular.

Although by far the least explored and least known planet up to a few years ago, the recent advances have been tremendous and it is probably fair to state that our current understanding of Mercury's deep interior is better than that of Venus and might probably reach the level of our knowledge of Mars once BepiColombo will return its data to the Earth. Spacecraft measurements alone, however, are not sufficient to reach this goal. A major problem is that direct experimental data about the high-pressure behaviour of putative bulk Mercury chemical compositions is very scarce. As a result, studies on Mercury's interior have had to either simplify interior property models, or use thermodynamic models to predict interior mineralogy based on experiments performed at conditions of pressure, temperature, composition, and oxygen fugacity far outside those invoked for Mercury. Additional data and insight are therefore needed on the behaviour of planetary materials at the high pressures and temperatures in the planet interior.

With COME-IN we aimed at advancing our understanding of Mercury by integrating complementary approaches from igneous petrology, high-pressure mineral physics, computational materials science, geodesy, and geodynamics in addition to using the constraints set by recent observational data. The ultimate goal was to gain deeper insight into the interior structure, composition and evolution of Mercury and to better understand the physical and chemical processes leading to the geological and magmatic diversity observed at the surface of Mercury. To achieve these objectives several complementary lines of investigation were integrated related to the crust, mantle and core of Mercury, including performing novel high-pressure experiments and developing advanced theoretical modelling. With this novel and interdisciplinary approach, based on fundamental science, we complement existing research initiatives in the frame of the MESSENGER and BepiColombo missions.

To reach our goal, a set of specific objectives was identified building upon the complementary expertise of the five partners. They are related to the primordial structure of Mercury after accretion, magmatic processes relevant to the differentiation and evolution of Mercury, the characterization of the physical properties and structure of the iron-rich core, and to the global interior structure and thermal evolution of Mercury. We provide below further background and a detailed description of those objectives.

A further objective of COME-IN was to stimulate the further development of expertise in the field of the interior structure and evolution of terrestrial planets of our solar system. This

enabled long-term collaborations between the different Belgian partners and facilitated reaching a critical mass allowing Belgium to play a leading international role in planetology. It also opened a new collaboration with VU University Amsterdam and created the possibility to develop a unique facility in Belgium to study materials at planetary pressure and temperature conditions. An additional intention of joining forces was to create a dynamic research environment attractive to young scientists.

2.1 Primordial silicate metal equilibration

2.1.1 Core-mantle partitioning of trace elements

The bulk composition of the core and the silicate shell of the planet is determined by the primordial structure of Mercury after accretion. The differences in FeO mantle contents and core masses between the terrestrial planets suggest that the oxygen fugacity (fO_2) during their differentiation likely varied significantly. MESSENGER data convincingly demonstrated that Mercury formed under very reducing conditions compared to the other terrestrial planets. The metal melt – silicate melt and sulfide melt – silicate melt partitioning of siderophile (iron-loving) and chalcophile (sulphur-loving) elements is a function of fO_2 and of the valence state(s) of these elements in silicate melts, but to date significantly fewer experimental datasets on metal-silicate and sulfide-silicate partitioning of elements are available at highly reducing conditions compared to less reducing conditions. We aimed to perform systematic experimental studies at pressures up to 6 GPa of the metal-silicate and sulfide-silicate partitioning behaviour of siderophile and chalcophile elements at very low fO_2 , using metals with variably amounts of dissolved Si and S, and to apply our results to core formation in Mercury. Besides considering the light elements Si and S, a further objective was constraining the partitioning of radioactive elements between the metallic core and the silicate portion of the planet, which is a crucial parameter for the thermal evolution of the planet.

2.1.2 The FeS layer at the core-mantle boundary

Based on MESSENGER chemical maps, particularly for sulfur, and experiments under reduced conditions, the intrinsic oxygen fugacity $\log(fO_2)$ of Mercury's mantle has been estimated to be in the range of IW-6.3 to IW-2.6, with a mean value of IW-5.4 \pm 0.4, with IW being the iron-wüstite redox equilibrium. Experiments on metal-silicate-sulfide equilibria conducted at these highly reducing conditions suggest the dissolution of important amounts of silicon (Si) in the Fe alloy during core formation. However at 4 – 7 GPa, which is the estimated pressure of Mercury's core-mantle boundary, there is a miscibility gap in the Fe-Si-S system causing the co-existence of two Fe-rich melts at sufficiently large light element concentrations: a FeS dominated sulfide melt and a Fe(Si) metallic melt. In the case of Mercury, if the bulk sulfur content of the planet was high enough at formation, a sulfide melt could have existed in addition to the metallic melts during its early differentiation and merged to form a buoyant layer at the top of the metal silicon-rich core. Early experimental data and geophysical data have suggested the potential existence of such an outer sulfide layer (solid or liquid) with a thickness below 200 km dependent on Mercury's S content. We investigated the likeliness of the existence of such a layer at the core-mantle boundary of Mercury by comparing new chemical surface data with geochemical models supported by high-pressure experiments under reducing conditions.

2.2 Mantle-crust evolution

2.2.1 Mantle melting conditions

To better understand magmatic processes relevant to the differentiation and evolution of Mercury, we aimed to investigate mechanisms of differentiation within the mantle and crust, and to embark on a study to determine the mantle source, composition and evolution of basalts and other lavas erupted at the surface. We thereto planned to conduct laboratory experiments at

high temperatures (1000-1600°C) and low to high pressure (1 atm to 4 GPa) to simulate the magmatic conditions from surface to mantle of the planet.

2.2.2 Mineralogy of the mantle and the crust

A further objective was to calculate the mineralogy and thermal and elastic properties of the mantle from its composition. Those properties are important for the general structure and thermal evolution of Mercury.

2.2.3 Crust density

The crust of Mercury was built over the first billion years of the planet by intense volcanic activity. Mantle melting and emplacement of lava to the surface produced a secondary magmatic crust varying spatially and over time in composition and mineralogy. Based on the expected crust mineralogy and density derived from MESSENGER X-ray and gamma-ray mapping, we calculated the thickness of the crust taking into account lateral variations of crustal density.

2.3 Core structure

2.3.1 Density and VP measurements of Fe-Si liquids at high pressure

In order to better characterize the physical properties and structure of the iron-rich core, COME-IN aimed at performing measurements of the density and melting behaviour of Fe-light element compositions at high pressure (4 – 25 GPa) and temperature, including quantification of the effect of the presence of nickel. In addition to experimental studies, a further objective was to complement these studies by ab initio calculations of the crystal structure and other properties of the inner core.

Since measurements of Mercury's rotation variations have convincingly demonstrated that Mercury's large metallic core is at least partially liquid (Margot et al. 2012), the physical properties of plausible liquid core alloys play a central role in modelling the interior structure of this planet. As a consequence of Mercury's low oxygen fugacity inferred from MESSENGER data, it is considered likely that Si, instead of S, is the dominant light element to alloy with Fe in the core. Before the COME-IN project, experimental data on the physical properties of Fe-Si liquid at high pressures, such as P-wave velocity (VP) and density, were sparse and inconsistent (for density) or unavailable (for VP) at the pressure regime relevant for Mercury's core. One of the objectives of the COME-IN project is to experimentally measure the VP and density of Fe-Si metallic liquid alloys at high pressure and to incorporate the results in interior structure models of the planet.

2.3.2 Core heat budget

Although rotation and the gravitational field of Mercury give insight into Mercury's interior structure, the thermal state of the core (and planet) and the radius of the inner core are not or only weakly constrained. A further constraint on the core can be obtained from the fact that Mercury currently has a global magnetic field and also had a magnetic field in the very early stages of its history. We studied interior structure models that allow for past- and present-day magnetic field generation and that agree with rotation measurements, gravity data, and deduced global radial contraction. Both models with and without Si as the main light element were considered. Those models put constraints on the inner core radius since it is required that those models allow for solid iron crystallization configurations that do not preclude present day magnetic field generation. To assess the relation between the structure of the core and the planet's capacity to produce a dynamo field, we modelled the thermal evolution of the core by calculating the evolution of the energy and entropy production in the core.

The large-scale and low-intensity characteristics of Mercury's magnetic field have been suggested to be due to a stably stratified liquid layer on top of a convecting liquid layer in

Mercury's core (Christensen, 2006). The origin of this stratification and convection must be understood in terms of the planet's thermal evolution. We developed three different methods to study the appearance and evolution of a stratified layer in the core. Motivated by the inferred low-oxygen fugacity and likely Si-rich core of Mercury, we examined whether the suggested present-day state of a stratified upper liquid layer and convecting lower layer can occur with a Fe-Si core-alloy, although Fe-S cores have also been studied. In contrast to S, Si does not significantly fractionate between solid and liquid metal such that compositional buoyancy plays an insignificant role for Si-rich cores. Consequently, the thermal evolution problem reduces to whether the heat from latent energy and secular cooling is sufficient to generate convection in the deeper region, yet insufficient to generate convection in an upper region of the core. To examine this scenario, a thermal evolution model was developed that deals with thermal fluxes that are subadiabatic (and negatively buoyant) in a consistent way, in contrast to most former thermal evolution models that adopt an adiabatic temperature profile for the entire core. This method uses an approximated analytical expression for the temperature in the conductive layer and ensures continuity of temperature and flux at the interface between the convective core and the stably stratified layer and conservation of total energy. In parallel, we also studied the thermal evolution of the (partly) stratified core based on the model of Greenwood et al. (SEDI and AGU 2018) developed for the Earth. Both solution methods use approximations to solve the partial differential heat equation. We also developed a fully numerical solution method for the exact governing equations. This method is expected to be more precise and is needed to test the adequacy of the two other methods but is much more complex to develop because of the inherent numerical difficulties in solving numerically diffusion problems. Depending on whether the core evolution has been coupled to a realistic model of the evolution of the mantle, results are described in Section 3.3 or Section 3.4.

2.3.3 Thermodynamic model of Fe-S-Si for the core

A precise thermodynamic description of materials in the core of Mercury is of fundamental importance for the interpretation of the data obtained from ground-based observations, the MESSENGER spacecraft and the upcoming BepiColombo mission. In order to build a model for Mercury's core and determine its melting temperature and thermo-elastic properties, thermodynamic models were constructed for different core compositions.

2.3.4 Composition and layered structure of the inner core

In the warm inner cores of terrestrial planets, stacking fault structures are expected to be common in addition to the classical structures (fcc, hcp, bcc) because of the high thermal energy available that can overcome the small differences in enthalpy with the classical structures. Observations of anisotropies in the seismic velocities in the Earth's core tend to support this idea. The prime candidate material of the Earths' inner core, hcp Fe, exhibits only moderate anisotropy and a vanishing orthogonal anisotropy at the core's high temperatures. We studied whether the presence of stacking faults can account for the observed anisotropy.

2.4 Models of the interior and evolution

2.4.1 Mercury's obliquity

The Cassini state is an equilibrium state in which the spin axis, the normal to the orbit, and the normal to the Laplace plane (an inertial plane which can be seen as the orbital plane averaged over the orbital precession period) are coplanar. An important constraint on the interior structure of Mercury is obtained from the measured obliquity of Mercury, the angle between the spin axis and orbit normal, since the obliquity is related to the polar moment of inertia if Mercury occupies the Cassini state. We developed a new extended model of Mercury's obliquity, which includes the effects of tides and of the precession of the pericenter. The model includes the variations (or nutations) in obliquity and the deviation with respect to coplanarity

induced by the slow precession of the pericenter. It also describes the constant shift over time in mean obliquity and deviation associated with the short-periodic tidal deformations of Mercury.

2.4.2 Global interior structure

We updated the core part of our interior structure models of Mercury to take into account the latest results about thermoelastic properties of liquid iron-sulfur and iron-silicon alloys at upper and middle Mercury core conditions (Terasaki et al. 2019). The resulting thermodynamic models predict thermoelastic properties for Fe-S and Fe-Si that are in good agreement with previously published data measured at pressures below and above that of Mercury's core. Hence, the new models provide for the first time a robust and concise description of the thermodynamic properties of the two most plausible end-member compositions of Mercury's liquid core.

We subsequently used those models to infer core structure properties from geodesy data (88 day libration amplitude, moment of inertia (MOI), and Love number k_2). Unlike previous estimations of the moment of inertia that were obtained by tracking features on Mercury's surface (Margot et al. 2012, Stark et al. 2015) the two most recent values were obtained from tracking MESSENGER orbiting Mercury (Genova et al. 2019, Konopliv et al. 2020). They both propose a significantly smaller value for the MOI than previous studies and for this reason are in favour of a smaller core. But a smaller core is at odds with the large core radius suggested by the large k_2 value reported in those two studies. Because of the large differences in the MOI in recent and previous studies we inferred core structure properties from the MOI and k_2 values of Genova et al. (2019) and Konopliv et al. (2020) as well as from the MOI value of Margot et al. (2012) and the k_2 value of Verma et al. (2016). For each set we used the 88 day libration amplitude of Margot et al. (2012).

2.4.3 Global thermal evolution

During the project duration, several studies were published in which new data for the libration and obliquity are presented. We consistently updated our models of the interior structure of Mercury to these data and assessed the consequences and consistencies of the different data sets.

2.4.4 Mantle convection

In order to construct global models of the evolution of the whole planet Mercury, we investigated the evolution of the mantle of Mercury, using a parameterized 1 dimensional model of mantle convection based on the work of Morschhauser et al. (2011) and Grott et al. (2011).

2.4.5 Rotational evolution

Motivated by the discovery of NASA's MESSENGER mission that significantly more large ancient craters are located on Mercury's Western Hemisphere than on the Eastern Hemisphere (Wieczorek et al. 2011), we examined if this observation can be explained by ancient impacting during a former different rotational state of Mercury.

3. METHODOLOGY, SCIENTIFIC RESULTS AND RECOMMENDATIONS

3.1 Primordial silicate metal equilibration

3.1.1 Core-mantle partitioning of trace elements

At VU Amsterdam, a first set of sixty-nine high pressure (P) – temperature (T) partitioning experiments was performed focusing on partitioning between silicate and iron-rich metals containing variable amounts of Si in the absence of sulphur (Steenstra et al. 2020b; and in revision). Oxygen fugacities ranged between 1 and 7 units below the iron-wüstite buffer (ΔW). Experimental pressures and temperatures ranged between 1 and 5 GPa and 1883 to 2273 K, respectively.

In addition, we experimentally studied the metal-silicate and sulfide-silicate partitioning behaviour of trace elements in reduced silicate melts over a wide range of S contents as a function of redox state at a pressure of 1 GPa and temperatures in the range 1833–1883 K. Silicate melt S contents ranged between ~ 0.5 and ~ 20 wt%, with a corresponding silicate FeO range of ~ 0.4 to ~ 17.5 wt%, in a fO_2 range between 1 and 9 log units below the iron-wüstite buffer.

Experimental run product compositions for the Amsterdam experiments were measured using electron microprobe analyses at Utrecht University and the University of Münster, as well as laser ablation – inductively coupled plasma – mass spectrometry (LA-ICP-MS) at the University of Münster.

Metal-silicate partition coefficient data from our new experimental data base (Steenstra et al. 2020b) indicate that the partition coefficient of FeO in silicate melts decreases significantly from reducing to highly reducing conditions under C-saturated conditions. It was found that at conditions more reducing than $\Delta W = -3$ to -4 , the metal-silicate partitioning behaviour of the majority of the siderophile elements deviates significantly from values corresponding to their expected valence state(s). These results indicate that the activity in metal of the elements considered, including that of Si itself, is decreased as a function of Si metal content, and a thermodynamic approach was used to quantify these effects. Interaction coefficients of trace elements in Si-bearing, Fe-rich alloys derived from the new experiments are in good agreement with previously proposed values at similar pressures below 5 GPa. However, interaction coefficients with Si obtained for C-free systems decrease within the 1 to 11 GPa range, suggesting extrapolation of lower-pressure parameters may yield erroneous results at much higher pressures. These new results provide an extensive experimental foundation for studies of Mercury's differentiation under (highly) reduced conditions, which we started to perform (Steenstra and van Westrenen, under revision).

Sulfide melt – silicate melt partitioning data (Steenstra et al., 2020a) reproduce the decrease of the S concentration at sulfide saturation (SCSS) with decreasing FeO contents down to ~ 3 wt%, as well as its strong increase at < 3 wt% FeO. At S contents exceeding $> 6-9$ wt% S, the FeO contents increase again. Results show that most elements (Mg, Ti, V, Cr, Mn, Cu, Zn, Se, Nb, Cd, Sb, Te, Ta, Tl, Pb and Bi) are more chalcophile than siderophile at reducing conditions, whereas Si, Co, Ni, Ga, Ge, Mo and W preferentially partition into Fe-rich melts instead of sulfide liquids. Silicon, Ti, Se, and Te preferentially partition into Fe-S over (Fe,Mg,Ca)-S liquids, whereas Mn, Zn and Cd are more compatible in the latter. As proposed in the literature, chalcophile elements such as Cu, Se and Te behave less chalcophile with increasing S concentrations of the silicate melt, whereas the opposite is observed for nominally lithophile elements such as Mg, Ca and Ti. This data set forms the basis for future models of the geochemical evolution of the Mercurian mantle in the presence of sulfide liquids.

3.1.2 The FeS layer at the core-mantle boundary

We investigated the likeliness of the existence of an iron sulfide layer (FeS matte) at the core-mantle boundary of Mercury by comparing new chemical surface data, obtained by the X-ray

Spectrometer onboard the MESSENGER spacecraft, with geochemical models supported by high-pressure experiments under reducing conditions. We built a new data set consisting of 233 Ti/Si measurements, which combined with Al/Si data show that Mercury's surface has a slightly subchondritic Ti/Al ratio of 0.035 ± 0.008 . Multiphase equilibria experiments showed that at the conditions of Mercury's core formation, Ti is chalcophile but not siderophile, making Ti a useful tracer of sulfide melt formation. We parameterized and used our partitioning data in a model to calculate the relative depletion of Ti in the bulk silicate fraction of Mercury as a function of a putative FeS layer thickness. By comparing the model results and surface elemental data we show that Mercury most likely does not have a FeS layer, and in case it would have one, it would only be a few kilometers thick (<13 km). We also showed that Mercury's metallic Fe(Si) core cannot contain more than ~ 1.5 wt% sulfur and that the formation of the core under reducing conditions is responsible for the only slightly subchondritic Ti/Al ratio of Mercury's surface.

3.2 Mantle-crust evolution

3.2.1 Mantle melting conditions

The MESSENGER spacecraft provided geochemical data for surface rocks on Mercury. We used the major element composition of these lavas to constrain melting conditions and residual mantle sources on Mercury. We combined modelling and high-temperature (1320–1580 °C), low- to high-pressure (0.1 to 3 GPa) experiments on average compositions for the Northern Volcanic Plains (NVP) and the high-Mg region of the Inter crater Plains and Heavily Cratered Terrains (High-Mg IcP-HCT). Near-liquidus phase relations showed that the S-free NVP and High-Mg IcP-HCT compositions are multiply saturated with forsterite and enstatite at 1450 °C – 1.3 GPa and 1570 °C – 1.7 GPa, respectively. For S-saturated melts (1.5–3 wt.% S), the multiple saturation point (MSP) is shifted to 1380 °C – 0.75 GPa for NVP and 1480 °C – 0.8 GPa for High-Mg IcP-HCT. To expand our experimental results to the range of surface compositions, we used and calibrated the pMELTS thermodynamic calculator and estimated phase equilibria of ~ 5800 compositions from the Mercurian surface and determined the P – T conditions of liquid–forsterite–enstatite MSP (1300–1600 °C; 0.25–1.25 GPa). Surface basalts were produced by 10 to 50% partial melting of variably enriched lherzolitic mantle sources. The relatively low pressure of the olivine–enstatite–liquid MSP seems most consistent with decompression batch melting and melts being segregated from their residues near the base of Mercury's ancient lithosphere. The average melting degree is lower for the young NVP (0.27 ± 0.04) than for the older IcP-HCT (0.46 ± 0.02), indicating that melt productivity decreased with time. The mantle potential temperature required to form Mercurian lavas and the initial depth of melting also decreases from the older High-Mg IcP-HCT terrane (1650 °C and 360 km) to the younger lavas covering the NVP regions (1410 °C and 160 km). This evolution supports strong secular cooling of Mercury's mantle between 4.2 and 3.7 Ga and explains why very little magmatic activity occurred after 3.7 Ga.

3.2.2 Mineralogy of the mantle and the crust

We examined XRS chemical maps of Mercury and identified average compositions for the various provinces. We experimentally investigated the phase equilibria of five S-free compositions. Experiments were performed from 1,480 to 1,100 °C at 1 kbar under reducing conditions similar to those of Mercury's mantle (4W-5, IW being the iron–wüstite buffer). All compositions fall within the forsterite stability field at low pressure. For the SiO₂-rich lavas of the NVP, stabilization of forsterite at the expense of orthopyroxene is due to the high Na₂O content of our starting composition (~ 7 wt%). The liquidus temperature ranges from 1,440 to 1,290 °C with decreasing MgO content. With decreasing temperature, residual melts become saturated first in diopside, followed by plagioclase, ortho-enstatite and tridymite.

We thus found a common crystallization sequence consisting of olivine, plagioclase, pyroxenes and tridymite for all magmas tested. Depending on the cooling rate, we suggest that lavas on

Mercury are either fully crystallized or made of a glassy matrix with phenocrysts. Combining the experimental results with geochemical mapping, we identified several mineralogical provinces: the Northern Volcanic Plains and Smooth Plains, dominated by plagioclase, the High-Mg province, strongly dominated by forsterite, and the Intermediate Plains, comprised of forsterite, plagioclase and enstatite. This implies a temporal evolution of the mineralogy from the oldest lavas, dominated by mafic minerals, to the youngest lavas, dominated by plagioclase, consistent with progressive shallowing and decreasing degree of mantle melting over time (Namur and Charlier 2017).

Knowledge of the mantle mineralogy and its thermal and elastic properties is important for the global structure and thermal evolution of Mercury. Based on an average chemical composition of the silicate crust, the mineralogy of the mantle and the crust can be determined as a function of depth by calculating thermodynamic phase equilibrium using programs such as *Perple_X* (Connolly 2005). As a preliminary work we calculated the thermoelastic properties of different Martian mantle compositions. The density and elastic properties of Mercury's thin mantle were determined as a function of depth with the same method.

3.2.3 Crust density and crustal production

The surface composition of the Mercurian volcanic crust was calculated using the most recent elemental composition maps produced from MESSENGER XRS data. We selected the pixels for which Mg/Si, Ca/Si, Al/Si and S/Si were measured. From those data, we produced >79,000 compositional groups of four pixels (0.5° latitude x 0.5° longitude). Each pixel group was assigned to the geochemical province in which it is located (NVP, SP, IcP-HCT, HMg), to which we attributed specific concentrations of minor elements (Ti, Mn, K). For Na, we considered that NVP lavas have high Na₂O contents (Na/Si = 0.20; ca. 7 wt% Na₂O), SP lavas have intermediate Na₂O contents (Na/Si = 0.14; ca. 5 wt% Na₂O) and IcP-HCT and HMg lavas have lower Na₂O contents (Na/Si = 0.06; ca. 2 wt% Na₂O). Elemental ratios were converted to oxide compositions assuming normalization to 100 wt%. Experiments in Fe-free systems at reducing conditions (<IW-5) show that sulfide saturation produces sulfide melt globules with an average composition of (Mg_{0.8}Ca_{0.2})S. We therefore recalculated S-free bulk compositions by subtracting Ca and Mg contents according to the bulk S content measured by MESSENGER before determining the silicate mineralogy of Mercurian lavas. In this study, we used the silicate mineralogy of the surface of Mercury for fully solidified magma. Mineral proportions were calculated using mass-balance between the stable liquidus phases obtained experimentally (plagioclase, quartz, forsterite, enstatite and diopside) and the bulk composition of lavas. Calculated mineralogy was converted to pore-free crustal density using the density of minerals at 25 °C. In order to obtain a complete mapping for the density of surface rocks (including regions where Ca/Si was not measured), we regressed an equation to calculate the rock density a function of Mg/Si and Al/Si as the only variables.

We then calculated the thickness of the crust taking into account lateral variations of crustal density. We show that the local thickness is correlated with the degree of mantle melting required to produce surface rocks. Low-degree melting of the mantle below the Northern Volcanic Plains produced a thin crust (19 ± 3 km) while the highest melting degree in the ancient High-Mg region produced the thickest crust (50 ± 12 km), disproving the hypothesis of mantle excavation by a large impact in that region. A correlation between crustal thickness and mantle melt production also exists for the oceanic crust on Earth and might be a common feature of secondary crust formation on terrestrial planets (Charlier et al., under revision).

3.3 Core structure

3.3.1 Density and VP measurements of Fe-Si liquids at high pressure

The VP and density of Fe-Si liquid metals at high temperatures (1400-1900 K) and high pressure (2-6 GPa) were measured in two separate experimental campaigns.

The VP was measured in-situ at beamline 16-BMB of the Advanced Photon Source (APS) synchrotron facility at the Argonne National Laboratory of the United States near Chicago. The sample energy-dispersive X-ray spectra (EDX) were used to determine the liquid state of the sample. The experimental temperature and pressure conditions were determined from the X-ray spectra (EDS) of alumina and boron-nitride (calibrant materials). The sample width was determined by in-situ radiographic imaging. The two-way travel time of 20, 25, and 30 MHz soundwaves through the sample, were used to determine the P-wave velocity (VP) of the sample.

The density experiments were performed by four of the five COME-IN partner teams at the European Synchrotron Radiation Facility (ESRF) in Grenoble, France. The angle-dispersive sample X-ray spectra (ADS) were used to determine the liquid state of the sample. The experimental temperature and pressure conditions were determined from the angle-dispersive X-ray spectra of platinum and boron-nitride (calibrant materials). In-situ X-ray absorption data at experimental conditions were used to determine the absorption of the sample (μ_{PT}) at experimental conditions. X-ray absorption data after the experiment determined the absorption (μ_{ρ}) of the recovered sample at ambient conditions. The density of the recovered sample at ambient conditions (ρ) was measured after the in situ analyses at the Institute de Physique du Globe de Paris (IPGP) by an hydrostatic weighing technique. The density at experimental conditions follows from $\rho_{PT} = \rho \cdot \mu_{PT} / (\mu_{\rho})$.

The compositions of recovered samples of both experimental campaigns were determined by electron microprobe analysis at the Institute for Mineralogy of the University of Münster, Germany.

The density measurements of Fe-Si metallic liquids show that Si significantly reduces the density of Fe-rich metallic liquids. The measured densities of the Fe-15wt%Si experiments are fairly consistent with available density measurement of Fe-17wt%Si in scientific literature by Yu and Secco (2008), but are lower than those obtained by some other studies (Sanloup et al., 2004; Tateyama et al., 2011). The densities reported in the latter studies are likely significantly too high.

The VP measurements show that Si significantly increases the VP of Fe-rich liquid metal. This is in strong contrast with the reducing effect of S on the VP of Fe-rich liquids in the examined pressures range (2-6 GPa) that was reported by other experimental studies (e.g. Nishida, 2013; Jing et al., 2014).

Motivated by the distinct influences of Si and S on the VP of Fe-rich metallic liquids, we studied if this difference can be used to constrain the composition of Mercury's core by future seismic data. We computed Mercury interior models and the seismic wave propagation through Mercury by an open source matlab code 'TTBOX' (Knapmeyer, 2004). This modelling effort is currently ongoing. Preliminary results indicate that the potential of distinguishing binary Fe-S and Fe-Si core alloys of Mercury by seismic data strongly depends on the extrapolation of the VP of these alloys up to the high pressure regime of Mercury's core, and on whether an inner core is present. If a significant inner core is present in Mercury, the strong difference in VP of these alloys at the lower range of core pressure will lead to a strong difference in the seismic travel time of P-waves through the outer core. If an inner core is absent, the deeper (high-pressure) part of Mercury's core, where the accurate experimental VP data are lacking, plays a significant role. For those scenarios, more accurate experimental data are likely required to further refine interior models of Mercury.

3.3.2 Core heat budget

The usual approach to study the thermal evolution of the core is based on the energy balance at the core-mantle boundary because, unlike for the mantle, a numerical resolution of the Navier-Stokes equations is not possible with a realistic value of the viscosity at the pressure and temperature conditions of the core. In order to evaluate whether a dynamo can operate in the liquid part of the core, the heat budget has to be considered together with the entropy budget

since the Ohmic dissipation generated by the currents related to the magnetic field is not part of the energy budget of the core. Dissipation in general does not appear in the energy budget since it is essentially energy converted within the core, but it does appear in the entropy budget. We considered the energy and entropy contributions from core secular cooling and crystallization of iron alloys. The core model is based on the energy and entropy budgets developed in the articles of Gubbins et al. (2003, 2004) and on the core structure and thermal state from Davies (2015).

Because models of the thermal evolution of the Earth's core are more developed than those for other terrestrial planets, the core model was first set up for the Earth to allow testing with models available in the literature. The impact of a high thermal conductivity on the Earth's core evolution was investigated with the conclusion that this high value does not allow for a dynamo action before inner core nucleation. The addition of light element exsolution (Badro et al. 2016) from the core to the mantle was considered as an additional core process. The energy and entropy core budgets showed that precipitation of magnesium is one of the largest entropy contributions and can power the dynamo before inner core formation, providing a potential solution to problems caused by high thermal conductivity for the thermal and compositional evolution of the core.

The model was then adapted to the core of Mercury. We evaluated a necessary condition for the existence of a dynamo for a set of Mercury interior models and considered two core radii in agreement with constraints from rotation and tides (1950 km and 2050 km, see also Section 3.4.2). The core is composed of iron and sulfur, with sulfur concentrations varying between 2-3 wt% in small Fe-S cores and about 5 wt% in large Fe-S cores (Dumberry et al. 2013, Rivoldini and Van Hoolst 2013, Deproost et al. AGU 2016).

Our study showed that powering a pure thermal dynamo during the whole evolution of Mercury requires a core-mantle boundary heat flux that is significantly larger than that predicted by mantle thermal evolution studies (about 10 mW/m²), and a core cooling rate at odds with the observed radial contraction of Mercury. The predicted large cooling rate and the resulting large core temperature imply a molten lower mantle for a significant part of Mercury's evolution, in contradiction with the early cessation of major effusive volcanism and crust formation episode. For both small and large cores, other energy and entropy sources are required to maintain convection and dynamo action up to this day. The addition of Si (5-10 wt%) to the core results in significantly larger amounts of latent heat generated upon Fe-Si freezing compared to sulfur and makes dynamo action possible during the whole evolution of the core. Dynamo action can also be extended to the present day if radioactive elements are present in the core with an abundance of about one tenth of the crustal abundance.

Thermal evolution studies of Mercury's core (Stevenson et al. 1983, Grott et al. 2011, Tosi et al. 2013), including those described above, show that the heat flux taken from the core by the mantle becomes rapidly subadiabatic. This supports the existence of a thermally stratified layer in the liquid outer core.

We developed three different thermal evolution models for the core that take into account the possible presence of this stably stratified layer. The different approaches taken are detailed below.

First we constructed a method in which the evolution of the average temperature in the conductive layer is controlled by the fluxes in and out the conductive layer. The temperature profile in the conductive layer is modelled by assuming a constant secular cooling in the conductive layer, from which an analytical temperature profile of the conductive layer is derived. The temperature profile of the entire core (the conductive and the convective region) is obtained from imposing conservation of energy.

In the second method based on the work of Greenwood et al. (2018a, 2018b), the evolution of the lower convective core is controlled by the energy balance at the interface between the convective and conductive layers. The temperature profile in the convective layer is taken to be adiabatic temperature and is determined from the heat equation in the conductive upper part of

the core. The position of the interface between both layers is fixed by the temperature and heat flux continuity conditions.

Comparisons of both methods show that the maximum difference in temperature between them are only a few degrees (0-5 K) throughout the entire evolution. The obtained temperature difference between the methods appears to be consistent with the inconsistency with regard to energy conservation in the method Greenwood et al. This insight and further examination suggests that the assumption of a constant secular cooling of the conductive layers in the first method leads to errors on the total thermal evolution of Mercury of below 2 K. For comparison, the model parameters that are of interest to these models lead to a variation of about 400 K of core temperatures among thermal evolution scenarios. This illustrates that the error that is caused by the simplification of the methodology in the first method is sufficiently small.

Within the second method, we determined how the presence of a stratified layer at the top of the core affects the thermal evolution of the core for different fixed heat fluxes at the core-mantle boundary. Conduction being less efficient than convection, a stratified layer cannot transport a significant secular cooling of itself in addition to the heat received from the lower convective core. As a result, the temperature at the core-mantle boundary is higher when a stratified layer is present. Since the energy going out of the core mainly comes from the convective region, the convective core cools faster the smaller it is (or the larger the stable layer is) for a given core-mantle boundary heat flux. This favours the buoyancy in the lower core making more entropy available for the dynamo in a stratified core.

Large Fe-S core models do not develop a bottom-up growing inner core. The cooling history of the convective core is almost insensitive to the core-mantle boundary heat flux. The smaller that heat flux is, the larger the stably stratified layer and the smaller the convective core. Although small convective cores cool faster for a given core-mantle boundary heat flux, their cooling rate is almost similar to those of larger convective cores corresponding to larger core-mantle boundary heat fluxes as they lose less energy through the core-mantle boundary. The difference in the temperature at the center of the core is smaller than 5 K for a core heat flux varying between 5 and 20 mW/m², while the stable layer thickness differs by several hundreds of km. The core is entirely conductive after at most 2.4 Gyrs because of either iron snow or stratification reaching the centre of the planet, depending on the core-mantle boundary heat flux.

In models with a small core, a solid inner core forms. Its nucleation time is similar whatever the subadiabatic core-mantle boundary heat flux, due to the same temperature evolution of the convective lower core before the inner core formation. The solid inner core growth generates buoyancy forces acting against stratification and the stable layer shrinks. As a result, the convective core cooling becomes more sensitive to the core-mantle heat flux and the difference between the present-day thermal state of this convective layer with and without a stratified layer is largely reduced: less than 0.5 K for the present-day central core temperature and less than 5 km the inner core size for a core heat flux between 10 and 20 mW/m².

The third method is a fully numerical solution method for the equations presented in the previous method. Because of the iterative approach of the second method, this numerical solution is expected to provide a deeper and more precise insight in the thermal evolution of the stratified core. In this method the heat equation is solved by the method of lines with a spatial discretisation of the stable layer. Numerical difficulties associated with the absence of a spatial convergence, stiffness of the diffusion equation, and a variable interface between the convective and conductive layers make this approach challenging. Preliminary results are promising and support the findings of the two other methods.

The core model was also used to study the thermal evolution and interior structure of the Moon. Unlike Mercury, the Moon does not have a present-day magnetic field, but evidence shows that an internally magnetic field was present between at least 4.2 and 3.56 Gyrs ago and likely continued at lower magnitude for billions of years. Large scale effusive volcanism came to an end about 1 Gyr after the formation of the Moon. Models without a solid inner core require a

core-mantle boundary temperature significantly above the mantle solidus in order to sustain a marginal dynamo until about 3.56 Gyrs and are therefore not in agreement with the observations. Unlike liquid core models, models that allow for inner core formation can have mantle boundary temperatures below the mantle solidus 1 Gyr after formation and agree with the timing of occurrence of the lunar dynamo. However, the predicted magnetic fields have magnitudes that are significantly below what is expected to explain the lunar magnetic records (Tikoo et al., 2017).

3.3.3 Thermodynamic model of Fe-S-Si for the core

A thermodynamic consistent model of Mercury's core is an important ingredient for modelling the internal structure and thermal evolution of the core. Considering Gibbs energy minimization, an equation of state was determined for the liquid pure iron phase based on existing melting data (Anzellini et al. 2013, Morard et al. 2018). From this equation of state thermo-elastic properties such as density or thermal expansion coefficient can be derived at Mercury's core temperature and pressure. Depending on the melting data set considered, values for the parameters entering the equation of state vary: between 145 GPa and 159 GPa for the bulk modulus, between 5 and 5.4 for its pressure derivative, and between 6.88 and 6.93 cm³/mol for the molar volume. This method can be extended to plausible core iron alloys with light elements such as sulfur or silicon in order to build a consistent thermodynamic model of Mercury's core and take into account the dependence of the core thermodynamic properties on core composition and temperature. We also developed a thermodynamic consistent model for Fe-Ni-S liquids based on recent laboratory experiments of the density and acoustic velocity of these alloys. Unlike density data, acoustic velocities cannot be described by a constant non-ideal excessive volume but requires it to be pressure dependent. A new model based on a pressure-dependent Margules formulation has been devised that agrees with both the density and acoustic velocity data. The new data and model show that models of Mercury assuming a Fe-S core would require more sulfur in their core to fit the average core density constraint than previous models. The older models neglected the non-ideal mixing of the Fe-S alloy, as it could not be modeled with the previous data set since densities had only been measured for one concentration of sulfur, and therefore significantly underestimated the compressibility of the alloy.

3.3.4 Composition and layered structure of the inner core

We performed ab initio calculations of the acoustic anisotropy of hcp crystals with stacking faults, including a model for random close-packed phased (i.e. an aperiodic, random stacking of close-packed planes). When focussing first on the pressure degree of freedom (temperature was kept at 0 K), we showed that – contrary to intuition – large amounts of stacking faults only increase the maximal acoustic anisotropy of the cold material. The cold hcp crystal has an acoustic anisotropy profile that is not too different from the one observed for the Earth's inner core, which is in agreement with previous studies. For both hcp and the randomly stacked model, the acoustic anisotropy was calculated also at 5000 K (and high pressure), to mimic inner core conditions. Including temperature in acoustic anisotropy calculations required code development, as well as a 100-fold increase in computational resources compared to the 0 K case. It turns out that the acoustic anisotropy of hot hcp Fe does not match at all with the observed anisotropy for the Earth's inner core. Yet, for the randomly stacked crystal, the agreement is very good. In a last step, we went beyond the model of one giant crystal with close-packed layers parallel to the equatorial plane, and considered distributions of misalignments with the North-South axis. This extra degree of freedom allows for a situation where the anisotropy profile of the model agrees perfectly with seismic observations. We therefore conclude that an aggregate of random close-packed iron crystals, aligned with their (111)-axes predominantly North-South but with an orientation distribution of 10°, and no

preferred orientation in the equatorial plane, is consistent with the observed seismic anisotropy, and this at the relevant temperature and pressure.

3.4 Models of the interior and evolution

3.4.1 Mercury's obliquity

Taking into account variations in obliquity and the deviation with respect to coplanarity induced by the slow precession of the pericenter, we showed that the polar moment of inertia estimated from the observed obliquity can be about 1% smaller than that deduced previously. This difference in moment of inertia is smaller than the current observational precision of a few % on the polar moment of inertia but of the order of precision that can be reached with BepiColombo mission ($\leq 0.3\%$). With our new model we also estimated the effect of tides on the spin axis orientation. We demonstrated that the neglect of tides in the interpretation of the obliquity leads to an error of 0.3% on the determination of the polar moment of inertia, but that the magnitude of the tides cannot be estimated from the spin axis orientation, because of its correlation with the polar moment of inertia. Our new model also allowed for the first time to put a lower bound on the tidal dissipation of Mercury. More precise estimates about the rheology of Mercury are expected from BepiColombo measurements.

The model developed for the orientation of a solid Mercury was extended to include the effect of the liquid outer core and solid inner core. It includes the internal gravitational and pressure couplings resulting from possible misalignment between the tidally deformed solid layers, and the viscous coupling at the core-mantle boundary in addition to the external torque by the Sun. It also takes into account the precession of the pericenter. The rotation of the fluid layer was modelled as a Poincaré flow. The effect of the partially molten core on the determination of the moment of inertia (up to a few percent) is larger than the expected future measurement precision ($\leq 0.3\%$), and will affect the interpretation of BepiColombo measurements.

3.4.2 Global interior structure

Our results show that models with and without an inner core are compatible with the most recent geodesy data. Fe-Si models with a completely molten core are, nevertheless, unlikely since they would require a core above the (not well known) lower mantle liquidus and therefore likely imply present-day surface volcanism, which disagrees with observations. Since it is difficult to explain the present-day core generated magnetic field of Mercury without a growing inner core, we only discuss results from models with an inner core.

Our result show that at 1 sigma Fe-S models have a core radius that is within 1972 km and 2000 km whereas for Fe-Si models the core can be about 20 km larger. Unlike for the core radius, geodesy data does almost not constrain the size of the inner directly. For a large inner core ($> \sim 1500\text{km}$), the gravitational and pressure coupling between the solid inner core and the silicate shell of the planet affect the 88 day libration amplitude (Van Hoolst et al. 2012) but the current uncertainty on the libration amplitude is still too large to make meaningful inferences about the inner core. The radius of the inner core follows therefore from the material properties (i.e. core liquidus) of the core and from its pressure and temperature conditions.

Our result show that for Fe-S models the inner core radius is below 1500 km (3 sigma) and the sulfur concentration in the core is below 6.5wt%. Models with the largest core radius have the smallest inner core (~ 200 km smaller) because of reasons of mass conservation. They are richer in sulfur which lowers the liquidus and moves the location where the core temperature drops below the liquidus to higher pressures.

Fe-Si models have an inner core radius that is between 1306 km and 2007 km and this range is almost independent of the core radius and measured k_2 values. The fraction of silicon in the core of those models is below about 18wt%. It is significantly larger than the required amount of sulfur to obtain the same average core density, because at a given light element concentration Fe-Si alloys are denser than Fe-S alloys.

Another question we addressed in this study is to assess the compatibility between the reported moment of inertia (MOI) and k_2 values. Our results showed that models inferred from the MOI- k_2 pair of Genova et al. (2019) are less likely than those obtained from the MOI- k_2 pair of Konopliv et al. (2019) and Margot et al. (2012)/Verma et al. (2016). This suggests that the MOI value of Genova et al. (2019) is likely too low and their k_2 value too high. Another possibility, which is not addressed in this study, is to allow for mantles with a lower rigidity (because of thermal or compositional effects). These models would have larger tidal deformations and thus allow for smaller and denser cores with a reduced MOI.

All in all, the core radius inferred from the recently measured MOI and k_2 does not significantly depart from that obtained from studies based on the MOI value of Margot et al. (2012).

3.4.3 Global thermal evolution

In a first study of the global thermal evolution (Knibbe and van Westrenen 2018), we showed that the excessive heat of the deep core redistributes to shallow core regions during periods of reduced heat flow out of the core. This propagates to higher temperatures of Mercury's mantle and outer core compared to results of previous models that keep the distribution of core heat fixed by an adiabat. As a consequence, S, which lowers the core melting temperature more drastically than Si, is not a necessary ingredient of Mercury's Fe-rich core for maintaining it partially liquid until the present. However, a solid inner core of substantial size likely exists in Mercury, if the core is of binary Fe-Si alloy. A substantial amount of Si suffices as Fe-core alloying element for it to remain partially liquid. Additionally, Si increases the latent heat release upon freezing such that core convection and present-day dynamo action can be driven by bottom up solidification of an Fe-Si core, while having an upper liquid core layer thermally stratified.

In addition to the first study, we also developed an alternative one-dimensional parameterised model of the evolution of the silicate shell and core, in which the second core model is used (Section 3.3). The mantle model is based on the work of Morschhauser et al. (2011) and Grott et al. (2011) with a lower convective layer and a stagnant lid that does not participate in convection. It is surrounded by the crust and a regolith layer. The crustal radioactive element concentrations are taken from Peplowski et al. (2011, 2012).

In a first step, we considered a constant crustal thickness and a core without thermal stratification. Large core models do not form a solid inner core and the core cooling is in agreement with contraction observations but the thermally driven dynamo only lasts until the Late Heavy Bombardment. In these models the present-day mantle is entirely conductive. In small core models, a solid inner core begins to grow after less than 200 Ma. A thermal and compositional dynamo is possible in the very beginning of the evolution and during the last part of the inner core formation, but convection in the core stops when iron snow reaches the inner core boundary after 2 Ga. In both large and small core models, the core temperature is sufficiently low to avoid melting of the lower mantle during the whole evolution, in agreement with surface observations about the formation of the crust. Convection in the core can be maintained in models with small core if radioactive elements are present in the core with an abundance of about 20% of the crustal abundances. Taking into account the heat generated by radioactive elements, the present-day inner core radius reaches about 1000 km and a dynamo is possible during the whole evolution. The mantle is still convecting today with a stagnant lid thickness of about 100 km.

Since geochemical observations by MESSENGER indicate that Si could be the main light element in the core, we considered models with silicon in the core in addition to sulfur. We showed that for core compositions of Fe-S-Si with 5-10 wt% Si, the energy and entropy produced in the core by the latent heat of freezing are larger than for Fe-S compositions by respectively 25% and 30%. The gravitational energy and entropy contributions are smaller because Si almost equipartitions in the solid and liquid phases of the core. The Fe-S-Si cores are,

at least partly, convective today and allow for a present-day dynamo. These models might be representative of Mercury, but still show some shortcomings. They, for example, have a molten lower mantle during a large part of the evolution of the planet, in contradiction with evidence of old major volcanic activity, and contract more during their evolution than is deduced from studies of surface tectonic features.

Convection in the core can be maintained in models with small core if radioactive elements are present in the core with an abundance of about 20% of the crustal abundances. Taking into account the heat generated by radioactive elements, the present-day inner core radius reaches 1200 km and a dynamo is possible during the whole evolution. The mantle is still convecting today with a stagnant lid thickness of about 100 km.

In a second step, the thermal evolution model has been improved to include the formation of the crust by partial melting of the mantle and the subsequent depletion of radioactive elements inside the mantle resulting from the melt migration to the surface. Furthermore, posterior considerations based on the idea of convective power showed that, in the models described above, the core would have been at least partly stratified during a large part of the core evolution. Therefore, the possibility of a thermal stratification in the upper part of the core has also been taken into account following the approach of Greenwood et al. (see section 3.3.2).

Both small core and large core models present an early stratification at the top of the core. In large core models, no inner core forms, the convection stops in the mantle after less than 2 Gyrs and only a pure thermal dynamo is possible during the first Myrs. Small core models still have a convective liquid layer several hundred of km thick today. The present-day inner core radius is about 1000 km and there is still a stratified layer at the top of the core of about 200 km. A dynamo is possible during the largest part of the evolution.

The presence of a stratified layer at the top of the core affects the core but also the mantle evolution. The higher temperature at the core-mantle boundary implies a larger heat flux from the core to the mantle. As a consequence the convective layer in the centre of the core cools faster while mantle cooling is slower. Convection is enhanced in the lower mantle and the melting period in the mantle is longer, creating more melt and a thicker crust. The fast cooling of the convective layer in the centre of the core generates buoyancy forces, enhancing entropy production and the possibility to drive a dynamo in the stratified core.

3.4.4 Mantle convection

We studied the convection in the lower mantle of Mercury in our one-dimensional parameterised global model of the planet. The mantle is conductive at the present day in large core models, taking or not stratification into account. In small core models, convection is still active today in the lower mantle if the core is partly stratified or if we add about 20% of radioactive crustal concentration into the core. In both cases, the mantle becomes warmer thanks to the larger heat flux coming from the core, enhancing convection in the lower mantle.

3.4.5 Rotational evolution

We developed a matlab code that spatially resolves the impact probability of an impactor, as a function of the orbital elements of Mercury and the impactor and the rotation rate of Mercury. This code is developed from scratch, based on pioneering mathematical works of Wetherill (1967) and Greenberg (1982). We additionally calculated the probability of Mercury's initial spin-orbit resonance capture as a function of Mercury's eccentricity, following recent novel methods of planetary rotational evolutions by i.e. Makarov (2012). Finally, we studied the stability of the relevant rotational states of Mercury (i.e the 1-1, 3:2 and 2:1 spin-orbit resonances) against the large impacts that Mercury has endured.

Our impact calculations show that the hemispherical asymmetry of ancient large craters on Mercury can be produced by impacting in a formerly synchronous rotation (1:1 spin-orbit resonance) or a former 2:1 spin-orbit resonance. The asymmetric crater distribution cannot be generated in the present-day 3:2 spin-orbit resonance. Hence, if a bias in the impacting is the

cause of the observed hemispherical asymmetry of ancient large craters, then Mercury must have been locked in a different rotational state during the ancient bombardment.

A former 2:1 spin-orbit resonance is a likely initial rotational state if Mercury initially had a rapid prograde rotation and an eccentricity similar to its present-day value. The 2:1 spin-orbit resonance would be easily destabilized by large impacts, such that a further deceleration to the present-day 3:2 spin-orbit resonance is a natural outcome. A former 1:1 spin-orbit resonance can also be obtained if the eccentricity was much lower when Mercury was decelerating in rotation. Only one or two large impacts (of which we have crater evidence) can have provided sufficient rotational momentum to cause a transition from a former synchronous rotation to Mercury's present-day 3:2 spin-orbit resonance. The Caloris Basin is the largest and among the most recent large craters on Mercury. The Caloris impact is therefore a feasible candidate to have initiated a transition from the former to the present-day rotational state of Mercury.

We conclude that it is likely that Mercury previously had a different stable rotational state. It is possible that the asymmetry in large ancient craters is a relic of impacting in a former 2:1 spin-orbit resonance or a former synchronous rotation of Mercury (Knibbe and van Westrenen, 2017).

4. DISSEMINATION AND VALORISATION

4.1 Presentations and abstracts

Baland R-M, Yseboodt M, Rivoldini A, Van Hoolst T, 2017. The influence of tides and of the precession of the pericenter on the orientation of the rotation axis of a solid Mercury. DDA 2017, London, UK

Baland R-M, Yseboodt M, Van Hoolst T, Rivoldini A, 2017. The influence of the fluid outer core and of the solid inner core on the orientation of the rotation axis of Mercury, EPSC, Riga, Latvia

Beuthe M, Rivoldini A, van Hoolst T, Charlier B, Namur O, 2018. Isostasy on Mercury in presence of lateral variations of crustal density. AGU Fall Meeting, Washington, USA

Cartier C, Namur O, Charlier B, Hammouda T, 2016. Elements partitioning during Mercury's two shells core formation. Goldschmidt Conference, Yokohama, Japan, 373

Cartier C, Namur O, Charlier B, 2017. No FeS layer in Mercury? Evidence from Ti/Al measured by MESSENGER. 48th Lunar and Planetary Science Conference, 1419

Cartier C, Namur O, Nittler LR, Charlier B, 2019. No FeS layer in Mercury: evidence from Ti/Al measured by MESSENGER. Goldschmidt Conference, Barcelona, Spain

Charlier B, Namur O, 2017. Mineralogical variations at the surface of Mercury. 48th Lunar and Planetary Science Conference, 1173

Charlier B, Beuthe M, Namur O, Rivoldini A, Van Hoolst T, 2018. Mantle melting productivity on Mercury and the relation with crustal thickness. AGU Fall Meeting, Washington, USA

Charlier B, Namur O, Cartier C, 2018. Perspectives on magmatic differentiation of Mercury. NASA Meeting on "Mercury: Current and Future Science of the Innermost Planet", Columbia, Maryland, USA

Charlier B, Beuthe M, Namur O, Rivoldini A, Van Hoolst T, 2019. Building the crust of Mercury. GeoMünster 2019, Münster, Germany

Deproost M-H, Rivoldini A, Van Hoolst T, 2016. Core thermal history and Magnesium exsolution. International School of Space Science (ISSS), Course on Planetary Interiors, L'Aquila, Italy

Deproost M-H, Rivoldini A, Van Hoolst T, 2016. Mercury's internal structure and core thermal evolution. DPS-EPSC, Pasadena, USA

Deproost M-H, Rivoldini A, Van Hoolst T, 2016. Mercury's interior structure constrained by geodesy and present-day thermal state. AGU, San Francisco, USA

Deproost M-H, Rivoldini A, Van Hoolst T, 2017. Thermal evolution constraints on the interior of Mercury. EGU, Vienna, Austria

Deproost M-H, Rivoldini A, Van Hoolst T, 2017. Thermal evolution and core stratification of Mercury. HP4, Göttingen, Germany

Deproost M-H, Rivoldini A, Van Hoolst T, 2018. Constraining the interior structure of Mercury by geodesy data. EPSC, Berlin, Germany

Deproost M-H, Rivoldini A, Van Hoolst T, 2018. Stratification of Mercury's core. HP4, Berlin, Germany

Deproost M-H, Rivoldini A, Van Hoolst T, 2019. Stratification in the core of Mercury. EPSC, Geneva, Switzerland

Jaeken J, Rivoldini A, Van Hoolst T, Van Speybroeck V, Waroquier M, Cottenier S, 2016. Ab initio prediction of sound velocities in planetary inner cores, DPG Spring Meeting, Regensburg, Germany

Knibbe JS, van Westrenen W, 2015. The Internal Configuration of Planet Mercury. LPSC, The Woodlands, USA

Knibbe JS, van Westrenen W, 2015. Mercury's Past Rotation and Cratering Distribution. LPSC, The Woodlands, USA

Knibbe JS, van Westrenen W, 2016, Mercury's Past Rotation and Cratering Distribution. NAC Conference, Veldhoven, the Netherlands

- Knibbe JS, van Westrenen W, Mercury's past rotation, in light of its large craters, ISSS Course on Planetary Interiors, L'Aquila, Italy, September 12-16 2016
- Knibbe JS, van Westrenen W, 2017. Mercury's Thermal Evolution and Magnetic Field Generation with an Fe-Si Core. 48th LPSC, The Woodlands, Texas, USA
- Knibbe JS, van Westrenen W, 2017. The thermal evolution and dynamo generation of Mercury with an Fe-Si core. EGU meeting, Vienna, Austria
- Knibbe JS, van Westrenen W, 2017. The thermal evolution and dynamo generation of Mercury with an Fe-Si core. 6th Joint Workshop of High Pressure, Planetary, and Plasma Physics (HP4), Göttingen, Germany
- Knibbe JS, Mercury's rotational evolution, in light of its large craters, KU Leuven, Leuven, Belgium, 23 February 2018
- Knibbe JS, 2018. Thermal Evolution of Mercury. Bepicolombo SWT#17, Braunschweig, Germany
- Knibbe JS, van Westrenen W, 2018. How to probe Mercury's origin. Nederlands Aardwetenschappelijk Congres (NAC), Veldhoven, Netherlands
- Knibbe JS, Luginbuel SM, Rivoldini A, Kono Y, Van Hoolst T, van Westrenen W, 2018. Future Seismic Constraints on Mercury's Core Composition. Mercury 2018, Baltimore, USA
- Knibbe J. S., Mercury, 2018. PhD defence, Amsterdam, the Netherlands
- Linsler S, Namur O, Albrecht M, Charlier B, Holtz F, McCammon C, 2015. Metal-silicate trace element partitioning at reducing conditions: Implications for Mercury's differentiation. GeoBerlin 2015, Germany
- Linsler SA, Namur O, Albrecht M, Charlier B, Holtz F, McCammon C, 2016. Metal-silicate trace element partitioning at reducing conditions: Implications for Mercury's differentiation. EMPG XV, ETH Zurich, Switzerland
- Morlok A, Charlier B, Klemme S, Namur O, Sohn M, Weber I, Stojic A, Hiesinger H, Helbert J, 2018. Remote sensing of planetary surfaces: spectroscopy of planetary analogs for the BepiColombo mission. European Planetary Science Congress 2018, Berlin, Germany
- Morlok A, Charlier B, Klemme S, Namur O, Sohn M, Weber I, Stojic A, Hiesinger H, Helbert J, 2018. Spectroscopy of synthetic planetary analogs for MERTIS on the BepiColombo mission. NASA Meeting on "Mercury: Current and Future Science of the Innermost Planet", Columbia, Maryland, USA
- Morlok A, Charlier B, Klemme S, Namur O, Sohn M, Weber I, Stojic A, Hiesinger H, Helbert J, 2018. Spectroscopy of planetary analogs for MERTIS on the BepiColombo mission. 49th Lunar and Planetary Science Conference
- Morlok A, Charlier B, Renggli C, Klemme S, Namur O, Carli C, Sohn M, Reitze M, Weber I, Stojic A, Hiesinger H, Helbert J, 2019. Infrared spectroscopy of synthetic planetary analogues for Mercury for the BepiColombo mission. European Planetary Science Congress, Geneva, Switzerland
- Morlok A, Charlier B, Renggli C, Klemme S, Namur O, Carli C, Sohn M, Reitze M, Weber I, Stojic A, Hiesinger H, Helbert J, 2019. Infrared spectroscopy of synthetic planetary analogues for Mercury for the BepiColombo mission. GeoMünster 2019, Münster, Germany
- Morlok A, Charlier B, Renggli C, Klemme S, Namur O, Carli C, Sohn M, Reitze M, Weber I, Stojic A, Hiesinger H, Helbert J, 2019. Infrared spectroscopy of experimental and synthetic planetary analogs for the BepiColombo mission to Mercury. 50th Lunar and Planetary Science Conference
- Namur O, Charlier B, Holtz F, 2015. Sulfur solubility in silicate melt at reducing conditions: Implications for Mercury's differentiation. GeoBerlin 2015, Germany
- Namur O, Collinet M, Charlier B, 2015. Experimental investigation of the mantle sources and melting conditions for Mercury's basalts. AGU-GAC-MAC-CGU Joint Assembly, Montréal, Canada

- Namur O, Collinet M, Charlier B, Holtz F, Grove TL, McCammon C, 2015. The mantle sources of surface lavas on Mercury. 46th Lunar and Planetary Science Conference, The Woodlands, Texas, USA
- Namur O, Charlier B, Holtz F, Cartier C, McCammon C, 2016. Sulfur solubility in reduced mafic silicate melts: Implications for the speciation and distribution of sulfur on Mercury. EGU, Vienna, Austria
- Namur O, Collinet M, Grove TL, Charlier B, 2017. Thermal evolution of Mercury's mantle as recorded by lava compositions. 48th Lunar and Planetary Science Conference, The Woodlands, Texas, USA
- Namur O, Charlier B, Cartier C, 2018. Carbon solubility in silicate melt under reducing conditions and the implications for Mercury. EMPG 16, Clermont-Ferrand, France
- Nittler LR, Cartier C, Charlier B, Crapster-Pregont E, Frank EA, Namur O, Starr RD, Vorburger A, Weider SZ, 2019. The surface abundance of titanium on Mercury. 50th Lunar and Planetary Science Conference, The Woodlands, Texas, USA
- Pirotte H, Cartier C, Namur O, Pommier A, Charlier B, 2019. The distribution of heat-producing elements during Mercury evolution. AGU Fall Meeting, Washington, USA
- Putter R, Steenstra ES, Seegers AX et al including van Westrenen W, 2017. Effects of fO_2 on Si metal-silicate partitioning of refractory and moderately volatile siderophile elements: Implications for the Si content of Mercury's core. Lunar and Planetary Science Conference, The Woodlands, Texas, USA
- Rivoldini A, Van Hoolst T, Noack L, Namur O, Charlier B, 2015. Constraining Mercury's interior structure with geodesy data and its present thermal state. MESSENGER – BepiColombo Joint Science Meeting, DLR Berlin, Germany
- Rivoldini A, Deproost M-H, Baland R-M, Van Hoolst T, Yseboodt M, Le Maistre S, Péters M-J, Dehant V, 2017. Nutational constraints on the interior structure of Mars. EPSC, Riga, Latvia
- Rivoldini A, Deproost M-H, Baland R-M, Van Hoolst T, Yseboodt M, Le Maistre S, Péters M-J, Dehant V, 2017. Nutational constraints on the interior structure of Mars. AGU, New Orleans, USA
- Rivoldini A, Deproost M-H, Van Hoolst T, 2018. Constraints on the lunar core composition and thermal state from geophysical data and thermodynamic properties of liquid iron-sulfur alloys. SEDI, Edmonton, Canada
- Rivoldini A, Beuthe M, Deproost M-H, Baland R-M, and Van Hoolst T, 2018. The interior structure of Mercury constrained by geodesy data. AGU, Washington, USA
- Rivoldini A., Deproost M.-H., and Van Hoolst T., 2019. Constraints on the lunar core composition and thermal state from geophysical data and thermodynamic properties of liquid iron alloys. UK SEDI, London, UK
- Seegers AX, Steenstra ES, Putter R et al. including van Westrenen W, 2017. The effect of Si and fO_2 on the metal-silicate partitioning of volatile siderophile elements: Implications for the Se/Te systematics of the bulk silicate Earth. Lunar and Planetary Science Conference 48, The Woodlands, Texas, USA
- Steenstra ES, Putter R, Seegers AX et al. including van Westrenen W, 2017. Significant non-linear pressure effects on interaction coefficients of siderophile elements in FeSi alloys: Implications for geochemical models of core formation in the Earth. Lunar and Planetary Science Conference 48, The Woodlands, Texas, USA
- Van Hoolst T, 2016. Interior and Tectonics of Mercury, SIMBIO-SYS team meeting, WG5 report, Rome, Italy
- Van Hoolst T, 2016. Gravity, tides and rotation of terrestrial planets and large icy satellites. ISSS Course on Planetary Interiors, L'Aquila, Italy
- Van Hoolst T, 2017. Geodesy and the Interior Structure of Planets and Moons of the Solar System. AGU fall meeting, New Orleans, Louisiana, USA
- Van Hoolst T, 2019. Planetary geodesy as a tool to study the deep interior of planets and satellites. medal lecture, EGU, Vienna, Austria. This invited lecture was given as part of the

ceremony related to the Runcorn-Florensky medal awarded to Tim Van Hoolst for “seminal contributions to the geodesy and geophysics of the terrestrial planets and satellites and for leadership in planetary geodesy”, which includes research on Mercury.

Van Hoolst T, 2019. The deep interior of terrestrial planets and icy satellites determined from planetary geodesy. UBern, Bern, Switzerland

Van Hoolst T, Beuthe M, Charlier B, Namur O, Rivoldini A, 2018. Variations in the thickness of Mercury's crust. SIMBIO-SYS team meeting, Kourou, French Guiana

Varatharajan I, Maturilli A, Helbert J, Ulrich G, Born K, Namur O, Kästner B, Hecht L, Charlier B, Hiesinger H, 2018. Bi-directional reflectance and NanoFTIR spectroscopy of synthetic analogues of Mercury: Supporting MERTIS payload of ESA/JAXA BepiColombo mission. European Planetary Science Congress, Berlin, Germany

Varatharajan I, Maturilli A, Helbert J, Ulrich G, Born K, Namur O, Kästner B, Hecht L, Charlier B, Hiesinger H, 2018. Nano-FTIR spectroscopy to investigate the silicate mineralogy of mercury analogues: supporting MERTIS onboard BepiColombo mission. NASA Meeting on “Mercury: Current and Future Science of the Innermost Planet”, Columbia, Maryland, USA

4.2 Organisation of Symposia

Session on Mercury's interior at the European Geosciences Union, Vienna, April 2017. The session focussed on COME-IN related themes of research. Co-conveners: T. Van Hoolst, B. Charlier.

Session on Dynamics of the mantle and core in the Earth and planetary bodies: from magma oceans to the present day at the European Geophysical Union, Vienna, April 2017. Co-conveners: O. Namur, C. Cartier.

4.3 Future projects and perspectives

As explained above, our results will increase the science return of MESSENGER and BepiColombo, missions in which the partners of this project are strongly involved. It will not only have a strong impact on our understanding of Mercury but will also be highly relevant for the mission preparation and science exploitation of this ESA cornerstone mission.

The European Space Agency (ESA) recently solicited the participation of the scientific community as Interdisciplinary Scientists or Guest Investigators in the BepiColombo mission, to augment the scientific return of the mission as a whole. BepiColombo is an interdisciplinary mission to the planet Mercury, carried out as a joint project between ESA and JAXA. It consists of two orbiters, the Mercury Planetary Orbiter (MPO) and the Mercury Magnetospheric Orbiter (MMO), which are dedicated to the detailed study of the planet and its magnetosphere. The BepiColombo mission was launched on 20 October 2018. Arrival at Mercury and start of the science exploitation phase are expected in December 2025 and April 2026, respectively. Bernard Charlier (in collaboration with Olivier Namur) has been awarded a position of Interdisciplinary Scientist (IDS) for the project “Petrological interpretations of the BepiColombo data” for an initial period of three years, renewable. IDSs are expected to focus their efforts on scientific cross-fertilisation and should not reflect instrument specific domains. IDSs are expected to be heavily involved with and/or have a leading role in the scientific activities of the mission. IDSs will take part in the analysis of data from different instruments on-board one or more elements of the mission. For these analyses they have the same data rights as the members of the Principal Investigator-led instrument consortia.

Jurriën Knibbe, who successfully defended his PhD thesis on Mercury at VU Amsterdam in 2018, was awarded a postdoctoral mandate with O. Namur and T. Van Hoolst at the KU Leuven in 2018-2019. Starting from October 2019, J. Knibbe works at KU Leuven and the Royal Observatory of Belgium with an FWO Seal of Excellence fellowship (T. Van Hoolst acts as supervisor). From July 2020 onwards, J. Knibbe will start a Marie Skłodowska Curie fellowship on Mercury research in the research team of T. Van Hoolst at the Royal Observatory of Belgium.

Those postdoctoral fellowships build further on the collaborations established within the COME-IN project.

5. PUBLICATIONS

- Armytage RM et al, including Knibbe JS (2018) White Paper on the case for Landed Mercury Exploration and the Timely Need for a Mission Concept Study, LPI white paper, <https://www.lpi.usra.edu/NASA-academies-resources/White-Paper-Landed-Mercury-Science.pdf>.
- Baland R-M, Yseboodt M, Rivoldini A, Van Hoolst T (2017) Obliquity of Mercury: influence of the precession of the pericenter and of tides. *Icarus* 291, 136-159
- Cremonese G et al., including Van Hoolst T (2019, submitted). SIMBIO-SYS: cameras and spectrometer for the BepiColombo mission. *Planetary and Space Science*, Special BepiColombo issue
- Cartier C., Namur O., Nittler L.R., Charlier B. (2019, revisions submitted) No FeS layer in Mercury: evidence from Ti/Al measured by MESSENGER. *Earth and Planetary Science Letters*
- Charlier B., Beuthe M., Namur O., Rivoldini A., van Hoolst T. (2019, revisions submitted) Mercury's crustal thickness controlled by mantle melt production. *Nature Geoscience*
- Charlier B., Namur O. (2019) Planet Mercury, *Elements* 15(1)
- This thematic issue of *Elements* contains 6 chapters and summarizes the most recent developments on planet Mercury in light of MESSENGER data and perspectives for the BepiColombo mission. It includes six chapters balanced between deep structures and surface processes, including insights from geophysics, geochemistry, igneous and experimental petrology and volcanology.
- Charlier B., Namur O. (2019) The origin and differentiation of planet Mercury. *Elements* 15: 9-14
- Deproost M-H, Rivoldini A, Van Hoolst T (2020) Thermal evolution of Mercury with a stratified upper core. In preparation
- Dumberry M and Rivoldini A (2015) Mercury's inner core size and core-crystallisation regime. *Icarus* 248(3), pp. 254-268, DOI: 10.1016/j.icarus.2014.10.038
- Genova A et al.
- Jaeken J, Cottenier S (2016) Solving the Christoffel equation: Phase and group velocities. *Computer Physics Communications* 20, 7445–451
- Jaeken J, Rivoldini A, Van Hoolst T, Cottenier S (2019, under revision) The effect of stacking faults on acoustic anisotropy of the inner core, *Nature Geoscience*
- Knibbe JS, and van Westrenen W. (2015), The interior configuration of planet Mercury, constrained by moment of inertia and planetary contraction, *Journal of Geophysical Research: Planets*, 120(11), 1904-1923
- Knibbe JS, and van Westrenen W (2017), On Mercury's Past Rotation, in Light of its Large Craters, *Icarus*, 281, 1-18
- Knibbe JS, and van Westrenen W (2018), The thermal evolution of Mercury's Fe-Si core, *Earth and Planetary Science Letters*, 482, 147-159
- Knibbe JS, Luginbuhl SM, Stoevelaar R, van der Plas W, van Harlingen DM, Rai N, Steenstra ES, van de Geer R, and van Westrenen W (2018), Calibration of a multi-anvil high-pressure apparatus to simulate planetary interior conditions, *EPJ Techniques and Instrumentation*, 5(5)
- Knibbe JS (2018), Mercury, PhD thesis, VU University Amsterdam, ISBN:9789090309675.
- Knibbe JS, Luginbuehl SM, Rivoldini A, Kono Y, Berndt-Gendes J, Van Hoolst T, Namur O, van Westrenen W (2019, under revision) High-pressure P-wave velocity measurements of Fe-Si and Fe-S liquids: implications for seismic observables of the Moon and Mercury, *Geophysical Research Letters*
- Namur O., Charlier B. (2017) Silicate mineralogy at the surface of Mercury. *Nature Geoscience* 10: 9-13
- Namur O., Charlier B., Holtz F., Cartier C., McCammon C. (2016) Sulfur solubility in reduced mafic silicate melts: Implications for the speciation and distribution of sulfur on Mercury. *Earth and Planetary Science Letters* 448: 102-114

- Namur O., Collinet M., Charlier B., Grove T.L., Holtz F., McCammon C. (2016) Melting processes and mantle sources of lavas on Mercury. *Earth and Planetary Science Letters* 439: 117-128
- Noack L., Rivoldini A., Van Hoolst, T (2016) Modeling the Evolution of Terrestrial and Water-rich Planets and Moons. *International Journal On Advances in Systems and Measurements* 9, 1&2, 66-76
- Steenstra ES, van Westrenen W. (2020, revised version under consideration) Metal-silicate partitioning of siderophile elements at reducing conditions: implications for core formation in Mercury and the Aubrite Parent Body. *Icarus*
- Steenstra ES, Trautner VT, Berndt J, Klemme S, van Westrenen W (2020b) Trace element partitioning between sulfide-, metal- and silicate melts at highly reduced conditions: insights into the distribution of volatile elements during core formation in reduced bodies. *Icarus* 335
- Steenstra ES, Seegers AX, Putter R, Berndt J, Klemme S, Matveev S, Bullock E, van Westrenen W (2020a) Metal-silicate partitioning systematics of siderophile elements at reducing conditions: a new experimental database. *Icarus* 335

Additional references

- Anzellini S., Dewaele A., Mezouar M., Loubeyre P., Morard G. (2013) Melting of Iron at Earth's Inner Core Boundary Based on Fast X-ray Diffraction. *Science* 340(6131), 464-466
- Badro J., Siebert J., Nimmo F. (2016) An early geodynamo driven by exsolution of mantle components from Earth's core. *Nature* 536, 326-328
- Christensen U. R. (2006) A deep dynamo generating Mercury's magnetic field. *Nature* 444, 21-28
- Connolly J. A. D. (2005) Computation of phase equilibria by linear programming: A tool for geodynamic modeling and its application to subduction zone decarbonation. *Earth and Planetary Science Letters* 236, 524-541
- Davies C. (2015) Cooling history of Earth's core with high thermal conductivity. *Physics of the Earth and Planetary Interiors* 24, 65-79
- Genova A., Goossens S., Mazarico E., Lemoine F. G., Neumann G. A., Kuang W., Sabaka T. J., Hauck II S. A., Smith D. E., Solomon S. C., Zuber M. T. (2019) Geodetic evidence that Mercury has a solid inner core. *Geophysical Research Letters* 46, 3625-3633
- Greenberg, R. (1982), Orbital interactions - a new geometrical formalism, *Astron. J.* 87, 184
- Greenwood S., Mound J., Davies C. (2018a) Thermal Stratification Beneath the Core Mantle Boundary. Poster at SEDI
- Greenwood S., Davies C., Mound J. (2018b) Thermal and Chemical History Modelling of a Stably Stratified Outer Core. An Open Source Python Package. Poster at AGU
- Grott M., Breuer D., Laneuville M. (2011) Thermo-chemical evolution and global contraction of Mercury. *Earth and Planetary Science Letters* 307, 135-146
- Gubbins D., Alfè D., Masters G., Price D., Gillan M. (2003) Can the Earth's dynamo run on heat alone? *Geophysical Journal International* 155, 609-622
- Gubbins D., Alfè D., Masters G., Price D., Gillan M. (2004) Gross thermodynamics of two-component core convection. *Geophysical Journal International* 157, 1407-1414
- Jing, Z. et al. (2013) Sound velocity of Fe-S liquids at high pressure: Implications for the Moon's molten outer core. *Earth and Planetary Science Letters* 396, 78-87
- Knapmeyer, M. (2004) TTBox: A MatLab Toolbox for the Computation of 1D Teleseismic Travel Times. *Seismological Research Letters* 75(2004):726-733
- Konopliv, A.S., Park, R.S., Ermakov, A.I. (2020) The Mercury gravity field, orientation, love number, and ephemeris from the T MESSENGER radiometric tracking data. *Icarus* 335 (2020) 113386

- Makarov, V.V., Berghea, C., Efroimsky, M. (2012) Dynamical evolution and spin-orbit resonances of potentially habitable exoplanets: the case of GJ 581d. *The Astrophysical Journal*, 761:83
- Margot J.-L., Peale S. J., Solomon S. C., Hauck II S. A., Ghigo F. D., Jurgens R. F., Yseboodt M., Giorgini J. D., Padovan S., D. B. Campbell D. B. (2012) Mercury's moment of inertia from spin and gravity data. *Journal of Geophysical Research* 117, E00L09
- Morard G., Boccato S., Rosa A. D., Anzellini S., Miozzi F., Henry L., Garbarino G., Mezouar M., Harmand M., Guyot F., Boulard E., Kantor I., Irifune T., Torcho R. (2018) Solving controversies on the iron phase diagram under high pressure. *Geophysical Research Letters* 45, 11074-11082
- Morschhauser A., Grott M., Breuer D. (2011) Crustal recycling, mantle dehydration, and the thermal evolution of Mars. *Icarus* 212, 541-558
- Nishida, K., Kono, Y., Terasaki, H., Takahashi, S., Ishii, M., Shimoyama, Y., et al. (2013). Sound velocity measurements in liquid Fe-S at high pressure: Implications for Earth's and lunar cores. *Earth and Planetary Science Letters* 362, 182-186
- Peplowski P. N., Evans L. G., Hauck II S. A., McCoy T. J., Boynton W. V., Gillis-Davis J. J., Ebel D. S., Goldsten J. O., Hamara D. K., Lawrence D. J., McNutt Jr. R. L., Nittler L. R., Solomon S. C., Rhodes E. A., Sprague A. L., Starr R. D., Stockstill-Cahill K. R. (2011) Radioactive Elements on Mercury's Surface from MESSENGER: Implications for the Planet's Formation and Evolution. *Science* 333(6051), 1850-1852
- Peplowski P. N., Lawrence D. J., Rhodes E. A., Sprague A. L., McCoy T. J., Denevi B. W., Evans L. G., Head J. W., Nittler L. R., Solomon S. C., Stockstill-Cahill K. R., Weider S. Z. (2012) Variations in the abundances of potassium and thorium on the surface of Mercury: Results from the MESSENGER Gamma-Ray Spectrometer. *Journal of Geophysical Research* 117(E00L04)
- Rivoldini A., Van Hoolst T. (2013) The interior structure of Mercury constrained by the low-degree gravity field and the rotation of Mercury. *Earth and Planetary Science Letters* 377-378, 62-72
- Sanloup, C., Fiquet, G., Gregoryanz, E., Morard, G., Mezoard (2004) Effect of Si on liquid Fe compressibility: Implications for sound velocity in core materials. *Geophysical Research Letters* 31, L07604
- Stark, A., et al. (2015) Mercury's rotational parameters from MESSENGER image and laser altimeter data: A feasibility study. *Planetary and Space Science* 117, 64-72
- Stevenson D. J., Spohn T., Schubert G. (1983) Magnetism and Thermal Evolution of the Terrestrial Planets. *Icarus* 54, 466-489
- Tateyama, R., E. Ohtani, H. Terasaki, K. Nishida, Y. Shibasaki, A. Suzuki, and T. Kikegawa (2011) Density measurements of liquid Fe-Si alloys at high pressure using the sink-float method, *Physics and Chemistry of Minerals* 38(10), 801-807
- Terasaki, H., Rivoldini, A., et al. (2019) Pressure and Composition Effects on Sound Velocity and Density of Core-Forming Liquids: Implication to Core Compositions of Terrestrial Planets. . Pressure and composition effects on sound velocity and density of core-forming liquids: Implication to core compositions of terrestrial planets. *Journal of Geophysical Research: Planets*, 124, 2272-2293
- Tikoo, S. et al. (2017) A two-billion-year history for the lunar dynamo. *Sci. Adv.* 2017;3:e1700207
- Tosi N., Grott M., Plesa A.-C., Breuer D. (2013) Thermochemical evolution of Mercury's interior. *Journal of Geophysical Research: Planets* 118, 2474-2487
- Van Hoolst T., Rivoldini A., Baland R.-M., Yseboodt M. (2012) The effect of tides and an inner core on the forced longitudinal libration of Mercury. *Earth and Planetary Science Letters* 333-334, 83-90
- Verma A., Margot J.-L. (2016) Mercury's gravity, tides, and spin from MESSENGER radio science data. *Journal of Geophysical Research: Planets* 121, 1627-1640
- Wetherill, G. W. (1967) Collisions in the asteroid belt, *J. Geophys. Res.* 72(9), 2429-2444

- Wieczorek, M. A., A. C. M. Correia, M. L. Feuvre, J. Laskar, and N. Rambaux (2011) Mercury's spin-orbit resonance explained by initial retrograde and subsequent synchronous rotation. *Nat. Geosci.* 5(1), 18–21
- Yu, X., & Secco, R. A. (2008) Equation of state of liquid Fe–17 wt%Si to 12GPa. *High Pressure Research* 28(1), 19–28.

6. ACKNOWLEDGEMENTS

Portions of this work were performed at HPCAT (Sector 16), Advanced Photon Source (APS), Argonne National Laboratory. The Advanced Photon Source is a U.S. Department of Energy (DOE) Office of Science User Facility operated for the DOE Office of Science by Argonne National Laboratory under Contract No. DE-AC02-06CH11357. HPCAT is supported by DOE-NNSA's Office of Experimental Sciences. Portions of this work were performed on beamline ID27 at the European Synchrotron Radiation Facility (ESRF), Grenoble, France.

The authors thank the European Space Agency (ESA) and the Belgian Federal Science Policy Office for their support in the framework of the PRODEX programme.